Improvements in the characterization of the crystalline structure of acid-terminated alkanethiol self-assembled monolayers on Au(111)

Mendoza, Sandra M.; Arfaoui, Imad; Zanarini, Simone; Paolucci, Francesco; Rudolf, Petra

Published in:
Langmuir

DOI:
10.1021/la0605539

Improvements in the Characterization of the Crystalline Structure of Acid-Terminated Alkanethiol Self-Assembled Monolayers on Au(111)

Sandra M. Mendoza,[†] Imad Arfaoui,[†] Simone Zanarini,[‡] Francesco Paolucci,*[,‡] and Petra Rudolf*[,†]

Materials Science Centre, University of Groningen, Nijenborgh 4, 9747AG Groningen, The Netherlands, and INSTM Unit of Bologna, Department of Chemistry "G. Ciamician", University of Bologna, via F. Selmi 2, 40126 Bologna, Italy

Received February 28, 2006. In Final Form: August 7, 2006

We report a study of acid-terminated self-assembled monolayers of alkanethiols of different length, 11-mercaptoundecanoic acid (11-MUA) and 16-mercaptohexadecanoic acid (16-MHDA), on Au(111). Scanning tunneling microscopy (STM), X-ray photoelectron spectroscopy (XPS), cyclic voltammetry (CV), electrochemical impedance spectroscopy (EIS), and contact angle techniques were used for characterization, and the results were compared with those obtained from *n*-alkanethiols of similar chain length, providing a detailed description of the two-dimensional crystalline structure. Molecular resolution STM images show that 11-MUA forms a dense-packed monolayer arranged in a $(\sqrt{3} \times \sqrt{3})R30°$ structure with a $c(2 \times 4)$ superlattice, where the simple hexagonal phase, the $c(2 \times 4)$ superlattice, and nonordered areas coexist. 16-MHDA assembles in a uniform monolayer with similar morphology to that of 11-MUA, but molecular resolution could not be reached in STM due to both the hydrophilicity of the acid groups and the poor conductivity of the thick monolayer. Nevertheless, the monolayer thicknesses estimated by XPS and electrochemistry and the highly blocking character of the film observed by electrochemistry as well as the low water contact angle are consistent with 16-MHDA molecules forming a compact monolayer on the Au(111) substrate with fully extended alkyl chains and acid groups pointing away from the surface. The results obtained for 16-MHDA were reproducible under different preparation conditions such as the addition or omission of acetic acid to the ethanolic solution. Contrary to other reports, we demonstrate that ordered acid-terminated self-assembled monolayers are obtained with the same preparation conditions as those of the methyl-terminated ones, without any additional treatment.

Introduction

In recent years self-assembled monolayers (SAMs) of alkanethiols on metal substrates have attracted the attention of many scientists in physics and chemistry due to their ability to form ordered organic films with well-defined composition and thickness.[1−23] They are potentially versatile building blocks for the development of advanced materials:[4] a proper selection of headgroups allows the chemical derivatization of a surface, and for this reason SAMs have been employed as a link path to graft molecules onto metal substrates, with the aim of modifying the surface properties.[5,6] In particular, acid-terminated alkanethiols are remarkably interesting due to their capability to react and/or strongly interact with many other chemical groups, leading to the functionalization of a surface with different molecules.

Several analytical techniques, such as spectroscopies,[1,2,7] contact angle,[8,9] ellipsometry and electrochemistry[10] have been used to study SAMs. As a result, there was a general agreement that long ($n > 6$) methyl-terminated alkanethiols on Au(111) form densely packed monolayers, with a chain tilt of ∼30° with respect to the surface normal and a structure with a $(\sqrt{3} \times \sqrt{3})$-$R30°$ lattice. Later helium diffraction[11] and STM[12] studies demonstrated the presence of a $c(4 \times 2)$ superlattice of the basic $(\sqrt{3} \times \sqrt{3})R30°$ structure. However, other authors claim that replacing the methyl termination by other functions does not always lead to the same organization and crystalline patterns and that variations in headgroups, chain length, and preparation conditions can give rise to different favored packing structures.[13−17]

The two-dimensional characteristics of acid-terminated alkanethiol SAMs have not yet been accurately described through STM studies. Furthermore, there is no clear agreement in the literature about what are the proper preparation conditions to obtain highly ordered acid-terminated monolayers. Nuzzo et al.[18] observed well-packed mercaptohexadecanoic acid monolayers

* Corresponding authors. Phone: +(31)50-3634736 (P.R.); +(39)051-2099460 (F.P.). Fax: +(31)50-363 4879 (P.R.); +(39)051-2099456 (F.P.). E-mail: p.rudolf@rug.nl (P.R.); francesco.paolucci@unibo.it (F.P.).

[†] University of Groningen.

[‡] University of Bologna.

(1) Zharnikov, M.; Grunze, M. *J. Phys.: Condens. Matter* **2001**, *13*, 11333.
(2) Duwez, A.-S. *J. Electron. Spectrosc. Relat. Phenom.* **2004**, *134*, 97.
(3) Smith, R. K.; Lewis, P. A.; Weiss, P. S. *Prog. Surf. Sci.* **2004**, *75*, 1.
(4) Love, J. C.; Estroff, L. A.; Kriebel, J. K.; Nuzzo, R. G.; Whitesides, G. M. *Chem. Rev.* **2005**, *105*, 1103.
(5) Berná, J.; Leigh, D. A.; Lubomska, M.; Mendoza, S. M.; Pérez, E.; Rudolf, P.; Teobaldi, G.; Zerbetto, F. *Nat. Mater.* **2005**, *5*, 704.
(6) Gu, T.; Whitesell, J. K.; Fox, M. A. *J. Org. Chem.* **2004**, *69*, 4075.
(7) Herdt, G. C.; Jung, D. R.; Czanderna, A. W. *Prog. Surf. Sci.* **1995**, *50*, 103.
(8) Bain, C. D.; Troughton, E. B.; Tao, Y.-T.; Evall, J.; Whitesides, G. M.; Nuzzo, R. G. *J. Am. Chem. Soc.* **1989**, *111*, 321.
(9) Faucheux, N.; Schweiss, R.; Lützow, K.; Werner, C.; Groth, T. *Biomaterials* **2004**, *25*, 2721.
(10) Porter, M. D.; Bright, T. B.; Allara, D. L.; Chidsey, C. E. D. *J. Am. Chem. Soc.* **1987**, *109*, 3559.
(11) Camillone, N.; Chidsey, C. E. D.; Liu, G.-Y.; Scoles, G. *J. Chem. Phys.* **1993**, *98*, 3503.
(12) Poirier, G. E.; Tarlov, M. J. *Langmuir*, **1994**, *10*, 2853.
(13) Alves, C. A.; Porter, M. D. *Langmuir* **1993**, *9*, 3507.
(14) Li, T.-W.; Chao, I.; Tao, Y.-T. *J. Phys. Chem. B* **1998**, *102*, 2935.
(15) Qian, Y.; Yang, G.; Yu, J.; Jung, T. A.; Liu, G.-Y. *Langmuir* **2003**, *19*, 6056.
(16) Berrena, E.; Ocal, C.; Salmeron, M. *J. Chem. Phys.* **1999**, *111*, 9797.
(17) Vericat, C.; Vela, M. E.; Salvarezza, R. C. *Phys. Chem. Chem. Phys.* **2005**, *7*, 3258.
(18) Nuzzo, R. G.; Dubois, L. H.; Allara, D. L. *J. Am. Chem. Soc.* **1990**, *112*, 558.
(19) Ito, E.; Konno, K.; Noh, J.; Kanai, K.; Ouchi, Y.; Seki, K.; Hara, M. *Appl. Surf. Sci.* **2005**, *244*, 584.
(20) Gorman, C. B.; He, Y.; Carroll, R. L. *Langmuir* **2001**, *17*, 5324.
(21) Dannenberger, O.; Weiss, K.; Himmel, H.-J.; Jäger, B.; Buck, M.; Wöll, Ch. *Thin Solid Films* **1997**, *307*, 183.
(22) Arnold, R.; Azzam, W.; Terfort, A.; Wöll, Ch. *Langmuir* **2002**, *18*, 3980.
(23) Willey, T. M.; Vance, A. L.; van Buuren, T.; Bostedt, C.; Nelson, A. J.; Terminello, L. J.; Fadley, C. S. *Langmuir* **2004**, *20*, 2746.

10.1021/la0605539 CCC: $37.00
Published on Web 11/23/2006

by infrared spectroscopy when using ethanol as a solvent for the SAM preparation. This was confirmed by the STM data of Ito et al.[19] and Gorman et al.[20] for the case of mercaptoundecanoic acid. However, other studies[21,22] demonstrated a high degree of disorder in mercaptohexadecanoic acid samples prepared only with ethanolic solutions and suggested that the quality of the surfaces can be improved with the addition of acetic acid to the solvent. In addition, Willey et al.[23] also claimed that well-ordered carboxylic-terminated SAMs of mercaptohexadecanoic acid can be formed by adding acetic acid, and they showed that rinsing in KOH causes the carboxylic group to be oriented much more upright. Finally, Wang et al.[24] argued that carboxylic-terminated SAMs are harder to control than methyl-terminated ones, and they proposed that addition of CF_3COOH to the ethanol followed by a rinse with NH_4OH improves the sample quality.

This report focuses on the crystalline structure of acid-terminated SAMs and compares them with methyl-terminated SAMs of similar length. For this purpose, four molecules have been selected: decanethiol (C10), hexadecanethiol (C16), mercaptoundecanoic acid (11-MUA), and mercaptohexadecanoic acid (16-MHDA). SAMs were characterized by X-ray photoelectron spectroscopy (XPS), cyclic voltammetry (CV), electrochemical impedance spectroscopy (EIS), and contact angle and scanning tunneling microscopy (STM) techniques. Since methyl-terminated SAMs on Au(111) have been extensively studied,[10,15,25−27] they have been chosen as the bench mark for comparison with carboxylic acid-terminated ones in our discussion.

By combining the above-mentioned experimental techniques, we have been able to show that carboxylic acid-terminated SAMs have equivalent chemical composition, thickness, and roughness as their methyl-terminated counterparts. Contrary to other studies,[21−24] we demonstrate that ordered and compact carboxylic acid-terminated SAMs can be obtained without any particular treatment such as the addition of acetic acid to the ethanolic alkanethiol solution.

Experimental Section

The Au(111)/mica substrates were prepared by vapor deposition of 150 nm gold film (purity 99.99%) onto freshly cleaved mica preheated at 375 °C for several hours in a custom-built high-vacuum evaporator (base pressure 10^{-7} mbar). The substrates were flame annealed in a hydrogen flame for 1 min and heated in UHV (10^{-9} mbar) for more than 3 h before use. After this treatment, no carbon and oxygen resulting from environmental contamination was detected by XPS and atomically flat Au(111) terraces with the $\sqrt{3} \times 23$ herringbone reconstruction were observed by STM. For the electrochemical experiments, gold films were similarly deposited also on silicon (111) with a Ti adhesive layer of 1 nm thickness.

11-MUA (97%) was purchased from Dojindo Co., 16-MHDA (90%) and C10 (96%) were purchased from Aldrich, C16 (95%) was purchased from Fluka, and acetic acid was purchased from Acros. All the compounds were used as received.

The gold substrates were immersed in a 1 mM solution of each alkanethiol for 1 day at room temperature. Ethanol was use as a solvent for the preparation of C10 and C16. 11-MUA and 16-MHDA solutions were prepared with both ethanol and chloroform,[6,28] and no difference was observed between samples immersed in either ethanol or chloroform. After removal of the samples from solution, they were rinsed with pure solvent or 5% acetic acid in ethanol and dried under an argon gas flow.

The STM study was performed using a Molecular Imaging STM with Pt/Ir mechanically cut tips. Images were recorded in the constant current mode with positive or negative bias voltage typically between 0.5 and 0.9 V and set point currents (I_{set}) lower than 25 pA, at room temperature in air. Data treatment included plane subtraction, smoothing, and adjustment of color scale and brightness to enhance the contrast.

The XPS measurements were performed using an X-PROBE Surface Science Laboratories photoelectron spectrometer with a monochromatic Al Kα X-ray source ($h\nu = 1486.6$ eV). The energy resolution was set to 1.2 eV to minimize data acquisition time, and the photoelectron takeoff angle was 37°. The binding energies were referenced to the Au $4f_{7/2}$ core level.[29] The base pressure in the spectrometer was 1×10^{-10} torr. A minimum number of scans was accumulated to avoid any X-ray damage.[8,30−32] Spectral analysis included a background subtraction and peak separation using mixed Gaussian−Lorentzian functions in a least-squares curve-fitting program (Winspec) developed in the LISE laboratory of the Facultés Universitaires Notre-Dame de la Paix, Namur, Belgium. The procedure consisted in fitting a minimum number of peaks that can reproduce the raw data and are consistent with the experimental resolution and the molecular structure of the film. All the measurements were performed on freshly prepared samples in order to guarantee the reproducibility of the results.

The electrochemical experiments were performed in unbuffered 0.1 M KCl Millipore aqueous solutions using a two-compartment electrochemical cell fitted with a saturated calomel electrode (SCE) and a platinum spiral as the counter electrode. Solutions were previously degassed by bubbling Ar through them. Experiments were carried out with an Autolab model PGSTAT 30 (Ecochemie).

The contact angle measurements of doubly distilled and demineralized water (Milli-Q, 18.0 MΩ) on the surfaces were carried out at room temperature by the sessile drop method[33] using a custom-built microscope−goniometer system. A 1.25 μL drop of the liquid was placed on a freshly prepared sample using a Hamilton microsyringe.

Results and Discussion

Scanning Tunneling Microscopy (STM). Figure 1 presents high-resolution STM images of a C10 monolayer. Figure 1a shows a molecularly resolved area where the molecules arrange in a hexagonal structure corresponding to the $(\sqrt{3} \times \sqrt{3})R30°$ lattice. A $c(4 \times 2)$ superlattice with respect to the fundamental hexagonal pattern is also visible due to variations in spot brightness, and the unit mesh is outlined to guide the eye. The cross section plot of the line superimposed in the image (Figure 1b) indicates that the brighter spots appear ~0.1 Å higher than the rest.[12,15] Figure 1c presents a 20×20 nm^2 image showing domains of molecules in which every domain has one of the three possible symmetry-equivalent orientations arising from the $c(4 \times 2)$ superlattice.[11,17] The darker areas are single-atom-deep etch pits in the gold terrace. These pits are vacancy islands of monatomic depth on the gold substrate and are induced by the dynamic self-assembly process that takes place during the formation of the monolayer in solution.[4]

Figure 2 shows STM images of 11-MUA, where molecular resolution was also achieved. Figure 2a displays a 27×27 nm^2

(24) Wang, H.; Chen, S.; Li, L.; Jiang, S. *Langmuir* **2005**, *21*, 2633.
(25) Wang, D. A.; Tian, F.; Lu, J. G. *J. Vac. Sci. Technol., B* **2002**, *20*, 60.
(26) Klein, H.; Blanc, W.; Pierrisnard, R.; Fauquet, C.; Dumas, Ph. *Eur. Phys. J. B* **2000**, *14*, 371.
(27) Lee, S.; Puck, A.; Graupe, M.; Colorado, R., Jr.; Shon, Y.-S.; Randall Lee, T.; Perry, S. S. *Langmuir* **2001**, *17*, 7364.
(28) Cecchet, F.; Rudolf, P.; Rapino, S.; Margotti, M.; Paolucci, F.; Baggerman, J.; Brouwer, A. M.; Kay, E. R.; Wong, J. K. Y.; Leigh, D. A. *J. Phys. Chem. B* **2004**, *108*, 15192.
(29) Moulder, F.; Stickle, W. F.; Sobol, P. E.; Bomben, K. D. *Handbook of X-ray Photoelectron Spectroscopy*; Physical Electronics, Inc., 1995.
(30) Heister, K.; Zharnikov, M.; Grunze, M.; Johansson, L. S. O.; Ulman, A. *Langmuir* **2001**, *17*, 8.
(31) Gonella, G.; Cavalleri, O.; Terreni, S.; Cvetko, D.; Floreano, L.; Morgante, A.; Canepa, M.; Rolandi, R. *Surf. Sci.* **2004**, *638*, 566.
(32) Laiho, T.; Leiro, J. A.; Heinonen, M. H.; Mattila, S. S.; Lukkari, J. *J Electron. Spectrosc. Relat. Phenom.* **2005**, *142*, 105.
(33) Mittal, K. L., Ed. *Contact Angle Wettability and Adhesion*; Utrecht, The Netherlands, 1993.

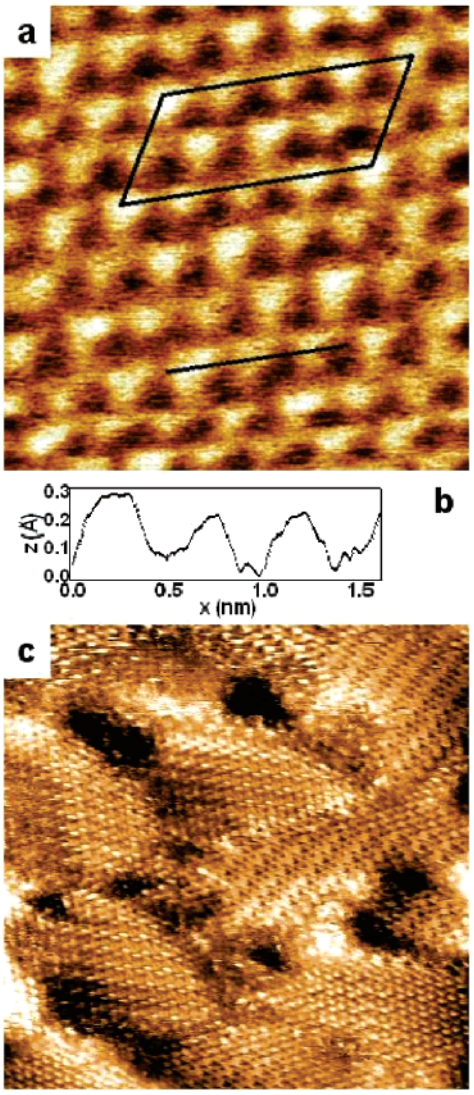

Figure 1. Scanning tunneling microscopy images of decanethiol (C10) on Au(111)/mica substrates: (a) 3.8×3.8 nm^2 image showing the $(\sqrt{3} \times \sqrt{3})R30°$ and $c(4 \times 2)$ lattices ($V_{bias} = 650$ mV, $I_{set} = 5$ pA). The $c(4 \times 2)$ unit mesh is outlined to guide the eye; (b) cross section plot of the line superimposed in the image; (c) 20×20 nm^2 image depicting domains of C10 and single-atom-deep etch pits ($V_{bias} = 500$ mV, $I_{set} = 20$ pA).

image with different morphologies. We can clearly recognize simple hexagonal domains such as "A". There are also ordered arrays of molecules forming domains "B" similar to the ones found on C10 (Figure 1c), which are a fingerprint of the $c(4 \times 2)$ superlattice. Other regions of type "C" are less defined and probably not ordered. Single-atom-deep etch pits in the gold terrace[4] are visible as well. Previous STM measurements carried out under nitrogen revealed a double-row structure in the 11-MUA SAM[20] that was not observed in the present study. We believe that this double-row arrangement corresponds to a nonresolved $c(4 \times 2)$ structure. A higher magnification image (Figure 2b) reveals that 11-MUA orders in a $(\sqrt{3} \times \sqrt{3})R30°$ packing with an average molecular distance of 5 Å. The hexagonal packing is clearly seen in the FFT-filtered image included as an inset. 11-MUA has a crystalline structure very similar to that of C10. However, while C10 presents large uniform areas with the same arrangement, 11-MUA forms a compact monolayer with a mixture of diverse morphologies and smaller ordered domains, which is a clear difference between acid- and methyl-terminated alkanethiols. Note that a poorer image resolution is achieved for

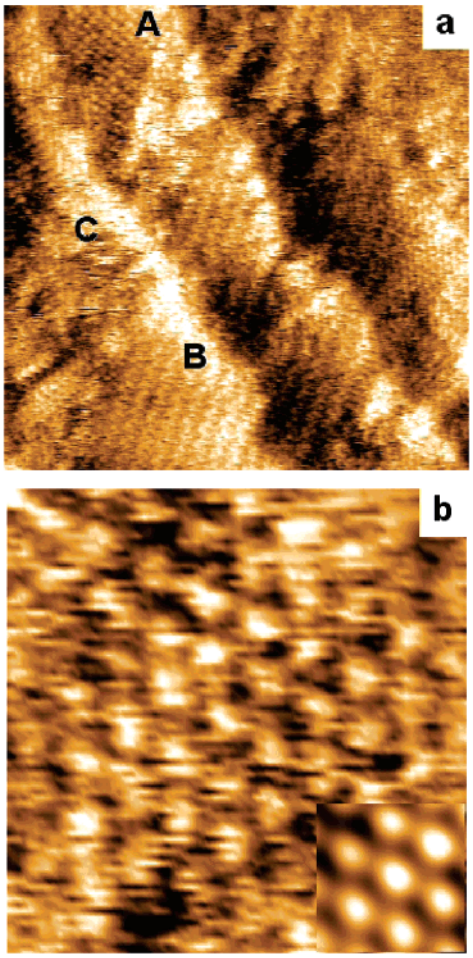

Figure 2. Scanning tunneling microscopy images of mercaptoundecanoic acid (11-MUA) on Au(111)/mica substrates: (a) 27×27 nm^2 image showing domains of molecules. A, simple hexagonal packing; B, $c(4 \times 2)$ arrangement; C, nonordered region ($V_{bias} = 800$ mV, $I_{set} = 5$ pA). (b) 4.1×4.1 nm^2 image showing the $(\sqrt{3} \times \sqrt{3})R30°$ structure ($V_{bias} = 800$ mV, $I_{set} = 5$ pA). Inset: 1.5×1.5 nm^2 section of the same image filtered by Fourier transformation showing the hexagonal lattice.

11-MUA than for C10 measurements, probably due to the presence of environmental contamination—such as water—adsorbed by the acid groups that interfere with the tip, changing its shape and perturbing the scanning process.

Figure 3 presents STM images of C16. Figure 3a shows a 30×30 nm^2 surface where ordered arrays of C16 and single-atom-deep etch pits in the Au terrace are seen. The distance between brighter spots of the ordered arrays suggests the presence of the $c(4 \times 2)$ reconstruction.[12,15] A higher resolution image (4×4 nm^2) shown in Figure 3b displays a highly ordered $(\sqrt{3} \times \sqrt{3})R30°$ arrangement with an average molecular separation of 5 Å, as for C10. The inset is part of the same image filtered by Fourier transformation to evidence the hexagonal lattice in more detail. These are the first STM images of C16 acquired with molecular resolution. To reach such a resolution it was necessary to work with a set point current not higher than 10 pA and bias voltage higher than 500 mV. Notice that SAMs with a long alkyl chain ($n > 14$) present a very poor conductivity. Bumm et al.[34] reported that a tunneling current lower than 1 pA should be used to obtain molecular resolution STM images of C16, which is not possible with current standard scanning tunneling microscopes. We ob-

(34) Bumm, L. A.; Arnold, J. J.; Dunbar, T. D.; Allara, D. L.; Weiss, P. S. *J. Phys. Chem. B* **1999**, *103*, 8122.

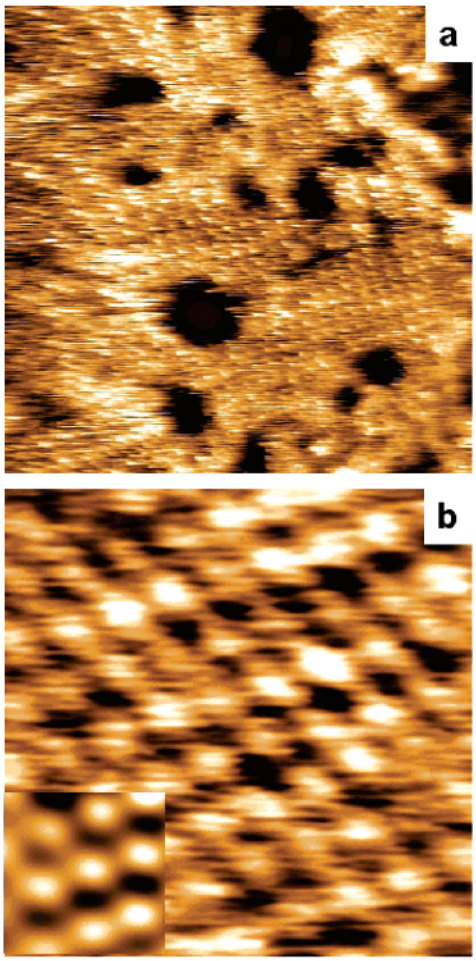

Figure 3. Scanning tunneling microscopy images of hexadecanethiol (C16) on Au(111)/mica substrates: (a) 30×30 nm^2 image showing domains of molecules ($V_{bias} = 700$ mV, $I_{set} = 5$ pA); (b) 4×4 nm^2 image showing the $(\sqrt{3} \times \sqrt{3})R30°$ structure ($V_{bias} = 550$ mV, $I_{set} = 10$ pA). Inset: part of the same image filtered by Fourier transformation showing the hexagonal lattice.

served that higher tunneling currents can be used to successfully observe the molecular structure of C16 if working with the proper bias voltage and tip shape. A few scans over the same area under the above-mentioned conditions were reproducible, but the quality of the image gradually decreased, probably due to damage of the monolayer and/or changes in the tip shape. A consequence of the low set current is a rather high noise level which does not allow us to observe a $c(4 \times 2)$ superlattice in clear detail.

Finally, STM results on 16-MHDA are shown in Figure 4. A 190×190 nm^2 scanned area reveals gold terraces covered by a uniform alkanethiol monolayer with single-atom-deep etch pits. Contrary to the systems described above, it was impossible to achieve molecular resolution in this case. The difficulty of imaging the 16-MHDA SAM arises from the poor conductivity of the thick organic film[34] and the hydrophilic nature of the acid groups that favor environmental contamination of the surface. Many samples were investigated, and they always presented the same characteristics everywhere, suggesting therefore that the monolayers are compact and uniform. As mentioned in the Introduction, previous studies reported that the addition of acetic acid to the preparation of 16-MHDA and a final rinse with KOH improve the monolayer order.[23] Samples prepared by this method were checked by STM (not shown); the results were similar to those described in Figure 4, but some regions presented evidence of contamination, probably due to difficulties in removing acetic

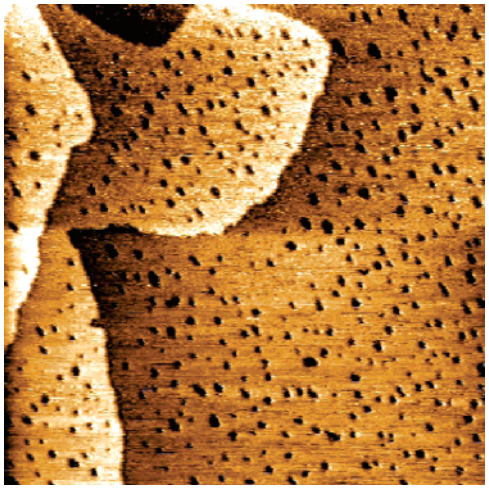

Figure 4. 190×190 nm^2 scanning tunneling microscopy image of mercaptohexadecanoic acid (16-MHDA) on Au(111)/mica substrates showing gold terraces covered by the SAM. Single-atom-deep etch pits are clearly seen. ($V_{bias} = 600$ mV, $I_{set} = 10$ pA).

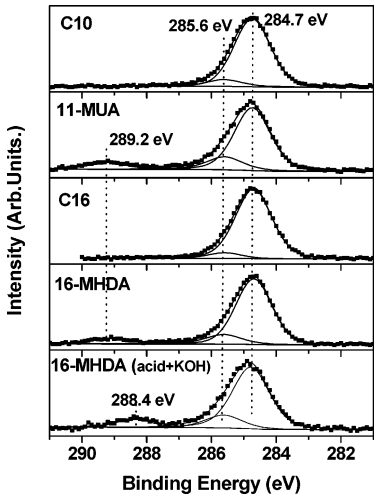

Figure 5. X-ray photoemission spectra of the C 1s core level region and fit of the experimental lines of self-assembled monolayers on Au(111)/mica substrates of decanethiol (C10), hexadecanethiol (C16), mercaptoundecanoic acid (11-MUA), mercaptohexadecanoic acid (16-MHDA), and 16-MHDA prepared with ethanol + acetic acid and rinsed with KOH.

acid molecules adsorbed on the surface. Thus, our observations do not support the conclusions of ref 23.

X-ray Photoelectron Spectroscopy (XPS). Figure 5 presents the C 1s core level region of the photoemission spectra of C10, 11-MUA, C16, and 16-MHDA as well as the fit of the experimental lines. In the case of C10 and C16, at least two components are needed to mathematically reconstruct the experimental line. They occur at binding energies of 284.7 and 285.6 eV and are unambiguously attributed to aliphatic carbon and carbon bound to sulfur, respectively.[29,35] The same features are found for 11-MUA and 16-MHA, where the peak at 285.6 eV is not only due to carbon bound to sulfur but also to the aliphatic carbon atom next to the carboxylic group. There is a third peak at 289.2 eV arising from carboxylic carbons. Peak positions, area ratios, and full width at half-maximum (fwhm) of the components are compatible with the stoichiometry of the alkanethiol molecules.

(35) Beamson, G.; Briggs, D. In *High-Resolution XPS of Organic Polymers*, The Scienta ESCA300 Database; John Wiley & Sons Ltd.: Chichester, U.K., 1992.

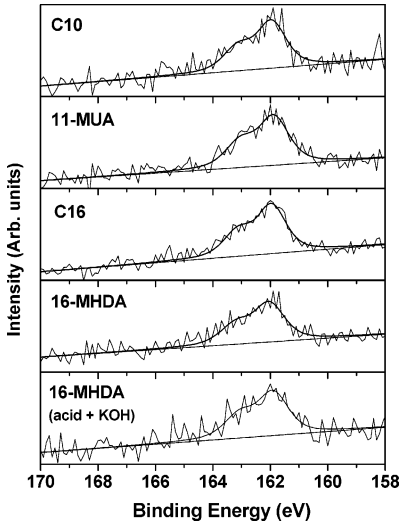

Figure 6. X-ray photoemission spectra of the S 2p core level region and mathematical reconstruction of the experimental lines of self-assembled monolayers on Au(111)/mica substrates of decanethiol (C10), hexadecanethiol (C16), mercaptoundecanoic acid (11-MUA), mercaptohexadecanoic acid (16-MHDA), and 16-MHDA prepared with ethanol + acetic acid and rinsed with KOH.

Samples of 16-MHDA prepared with a solution of acetic acid/ethanol and rinsed in KOH were investigated by XPS, and the C 1s region is also included in Figure 5 (16-MHDA acid + KOH). Peak positions and fwhm of the C 1s aliphatic components (at 284.7 and 285.6 eV binding energy, respectively) are identical to the previously discussed cases, and there is no evidence of a different chemical environment in aliphatic chains of 16-MHDA samples prepared with or without acetic acid, in contrast with the results obtained by Willey et al.[23] Hence, there is no indication of disorder in the monolayer produced without the addition of acetic acid. Carboxylate carbons appear at 288.4 eV, i.e., shifted to lower binding energy with respect to carboxylic groups due to charge-transfer and screening effects induced by the interaction between carboxylate groups and K^+ ions. The peaks at 288.4 and 285.6 eV binding energy are slightly more intense than expected when taking into account the stoichiometry of the molecule, suggesting the presence of residual acetic acid or acetate species. The potassium signal (not shown) appears as a doublet with the $2p_{3/2}$ maximum at 293.1 eV binding energy, and its area is in stoichiometric ratio with the C 1s area of the carboxylate group.

The S 2p core level region of the photoemission spectra of the four samples is presented in Figure 6. In particular, for the case of 16-MHDA we present the S 2p core levels of both the sample prepared only with ethanol and the sample prepared with ethanol + acetic acid and rinsed with KOH. All the S 2p spectra of carboxylic-terminated SAMs are identical to their methyl-terminated counterparts: all spectra are characterized by a doublet with maximum at 162.0 eV binding energy, an intensity ratio of 1:2, and a fwhm of 1.2 eV. There was no evidence of free (163.5 eV) or oxidized sulfur (168 eV)[29] in any sample, contrary to what was reported by Wang et al.[24] who observed unbound thiols in carboxylic acid-terminated SAMs prepared only with ethanol.

Our observations suggest no difference between SAMs prepared with or without acetic acid plus KOH rinsing, and we conclude that 16-MHDA SAM prepared only with ethanol presents the same chemical characteristics as C16 or 11-MUA, so the special preparation treatment with acetic acid plus KOH rinsing is not necessary to achieve an improvement.

The intensity of the signal produced by gold photoelectrons is attenuated by the alkanethiol monolayer, and this attenuation depends mainly on the SAM thickness: the thicker the film, the larger the substrate signal attenuation. Thus, XPS measurements are a good alternative to estimate the thickness of an alkanethiol monolayer. In the present work, we estimate the SAM thicknesses via the Au 4f core level assuming that the gold peak intensities follow the equation[36,37]

$$Au_1 = Au_0\, e^{-d/(\lambda \sin \varphi)}$$

where Au_1 is the intensity of gold photoelectrons attenuated by the SAM, Au_0 is the intensity from clean gold, d is the SAM thickness, λ is the attenuation length (reported as 42 ± 1.4 Å for alkanethiols on gold[36]), and φ is the takeoff angle. Thicknesses calculated by this method are presented in Table 1.

Table 1. SAM Thicknesses Estimated by the Attenuation of the Au 4f Signal

monolayers	C10	11-MUA	C16	16-MHDA
thickness (Å)	13 ± 2	15 ± 3	19 ± 3	19 ± 3

The results are in good agreement with previous ellipsometry studies on methyl-terminated alkanethiols[11,27,38] and with the calculated values taking into account the C−C distance of fully extended alkyl chains with 30° tilt with respect to the substrate normal.

In addition, the attenuation of the S 2p signal indicates that the sulfur atoms are not exposed to the surface but are at the bottom of the SAM. The relative attenuation of the sulfur signal was similar for C16 and 16-MHDA and larger than that for C10 or 11-MUA. This observation can be only explained if we consider that the alkanethiols form a compact film in all four cases.

Cyclic Voltammetry (CV) and Electrochemical Impedance Spectroscopy (EIS). Figure 7 shows the CV curve obtained for either 11-MUA (red full line) or 16-MHDA (blue dotted lines) SAMs on gold electrodes in a 2 mM $[Fe(CN)_6]^{3-/4-}$ aqueous solution (i.e., a 1 mM solution of both $[Fe(CN)_6]^{3-}$ and $[Fe(CN)_6]^{4-}$). For comparison the response of the bare gold electrode is also plotted (black short dashed line).

In the presence of either the 11-MUA or the 16-MHDA SAM, the faradaic current associated with the redox processes involving $[Fe(CN)_6]^{3-/4-}$ is largely suppressed and, together with the observed mostly capacitive behavior, testifies for the highly blocking character of the SAMs.[39] Not unexpectedly, the blocking effect of SAM is significantly larger in the case of the thicker 16-MHDA SAM than for 11-MUA.[40] Furthermore, the absence of peak-shaped morphology for both films, which is usually associated to a large contribution from defect sites or permeation,[41] is indicative of well-packed SAMs. On the other hand, the sigmoidal behavior observed at potentials close to the standard potential of the $[Fe(CN)_6]^{3-/4-}$ redox couple (see Figure 7, parts a and b) is pointing to the presence of kinetically active pinhole-like defects[42] that, by comparison with the response of the bare gold electrode, were estimated to cover less than 0.2% of the electrode surface.[39]

The highly blocking character of the SAMs was also assessed by performing an EIS analysis under the above conditions.[43] In

(36) Bain, C. D.; Whitesides, G. M. *J. Phys. Chem.* **1989**, *93*, 1670.
(37) Laibinis, P. E.; Bain, C. D.; Whitesides, G. M. *J. Phys. Chem.* **1991**, *95*, 7017.
(38) Chailapakul, O.; Sun, L.; Xu, C.; Crooks, R. M. *J. Am. Chem. Soc.* **1993**, *115*, 12459.
(39) Finklea, H. O. In *Electroanalytical Chemistry*; Bard, A. J., Rubinstein, I., Eds.; Marcel Dekker: New York, 1996; Vol. 19, pp 109−135.
(40) Terrettaz, S.; Becka, A. M.; Miller, C. *J. Phys. Chem.* **1995**, *99*, 11216.
(41) Diao, P.; Jiang, D.; Cui, X.; Gu, D.; Tong, R.; Zhong, B. *J. Electroanal. Chem.* **1999**, *464*, 61.
(42) Amatore, C.; Saveant, J.-M.; Tessier D. *J. Electroanal. Chem.* **1983**, *147*, 39.

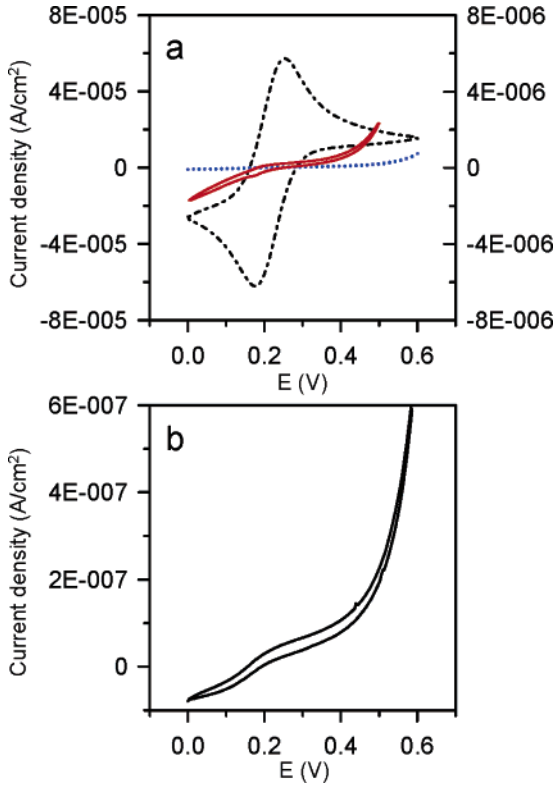

Figure 7. (a) CV curves of an aqueous solution of 2.0 mM $[Fe(CN)_6]^{3-/4-}$, 0.1 M KCl on a bare gold electrode (black short dashed line) (left scale); on a mercaptoundecanoic acid (11-MUA)-modified gold electrode [on Si(111)] (red full line); on a mercaptohexadecanoic acid (16-MHDA)-modified gold electrode [on Si(111)] (blue dotted line) (right scale); (b) enlarged view of CV curve of an aqueous solution of 2.0 mM $[Fe(CN)_6]^{3-/4-}$, 0.1 M KCl on a 16-MHDA-modified gold electrode [on Si(111)].

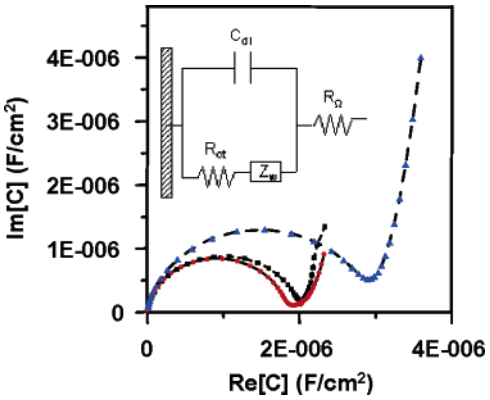

Figure 8. Complex capacitance plots (c-plots) recorded on a mercaptoundecanoic acid (11-MUA)-modified gold electrode (▲); on a mercaptohexadecanoic acid (16-MHDA)-modified gold electrode (on mica) (■), or on a 16-MHDA-modified gold electrode [on Si(111)] (●), in a 2.0 mM $[Fe(CN)_6]^{3-/4-}$, 0.1 M KCl aqueous solution, at 0.18 V. Inset: Randles' equivalent circuit.

Figure 8, the complex capacitance C measured for the various films at the open-circuit potential, which coincides in the present conditions with the standard potential of the $[Fe(CN)_6]^{3-/4-}$ redox couple (0.18 V), is displayed (c-plot).

Herein $C = 1/j\omega Z$, where Z is the interface (complex) impedance (a parametric function of the frequency f), $j = \sqrt{-1}$, and ω is the angular frequency ($= 2\pi f$). Notice that a semicircle in the c-plot is the expected response of a blocked electrode whose electric response to the sinusoidal potential perturbation is dominated, in the medium−high-frequency range, by the interface capacitance C ($= C_{dl}$) arranged in series with the electrolyte resistance R ($= R_\Omega$). The double-layer capacitance in the c-plot corresponds to the intercept of the semicircle onto the real axis.[44] At lower frequencies (frequency decreases from left to right in the plots of Figure 8), the contribution to the total interfacial impedance from electron-transfer processes involving the redox probe is also measured, possibly coupled to mass transport effects. The latter interfacial phenomena correspond, in the frame of the Randles equivalent circuit description of the electrochemical interface (see the inset in Figure 8), to the charge-transfer resistance R_{ct} and the Warburg impedance Z_W, respectively, and are responsible for the increase of complex capacitance observed at low frequencies in the plots of Figure 8. Inspection of Figure 8 would therefore confirm that a significantly lower C_{dl} value is obtained in the case of 16-MHDA films with respect to the 11-MUA ones. Furthermore, also in line with the voltammetric results (not shown), very similar C_{dl} values are obtained for the 16-MHDA films onto either mica or Si(111) substrates.

The electrical response of the interface was quantitatively described using the equivalent circuit[44] shown in Figure 8, and the electrical parameters were evaluated by fitting procedures, using the constrained nonlinear least-squares method (CNLS) method described by Boukamp.[45] From the best fit values for C_{dl} (3.1 and 2.0 μF cm^{-2} for 11-MUA and 16-MHDA, respectively), the average thickness of the SAMs was obtained within the Helmholtz capacitor approximation of the double layer, i.e., $d = \epsilon\epsilon_0/C_{dl}$. Assuming an average dielectric constant of the organic layer $\epsilon = 4.5 \pm 0.5$,[39] $d = 13 \pm 2$ and 20 ± 3 Å for 11-MUA and 16-MHDA SAMs, respectively, in rather good agreement with the values obtained by XPS.

Furthermore, from the value of R_{ct} measured at E_{oc}, the apparent standard rate constant value for the electron-transfer process involving the redox couple was estimated using the following relationship: $k^0 = (RT/n^2F^2AC_0)(1/R_{ct})$.[44] From the value for R_{ct} measured at E_{oc}, the apparent standard rate constant values for the electron-transfer process at the 11-MUA and 16-MHDA SAMs were 1.1×10^{-6} and 4.4×10^{-8} cm s^{-1}, respectively, in very good agreement with the CV behavior. Assuming that the electron transfer does occur via nonresonant through-bond tunneling, i.e., the rate decreases exponentially with the chain length, $k_{SAM} = k_{Au}\, e^{-\beta n}$,[46] the electronic tunneling factor per methylene unit obtained by comparing the above two k_{SAM}'s is 1.07, in very good agreement with the reported values for β.[39]

Contact Angle. The wettability of both acid- and methyl-terminated alkanethiols was investigated by measuring the contact angle of water on freshly prepared samples. The values, determined as the average of three identically prepared samples, where at least three points on each one were measured, are presented in Table 2. The high contact angle of 109° and 111° for C10 and C16, respectively, testifies to the hydrophobic nature of methyl-terminated monolayers. In contrast, both 16-MHDA (prepared with or without acetic acid + KOH rinse) and 11-MUA present very low contact angles, lower than 12° or 10°, respectively, when measured immediately after deposition. Water droplets deposited on acid-terminated SAMs spread very fast, making it difficult to determine an accurate contact angle value.

(43) Bard, A. J.; Faulkner, L. R. *Electrochemical Methods*; Wiley: New York, 2001.

(44) Barsoukov, E., MacDonald, R. J., Eds. *Impedance Spectroscopy. Theory, Experiment, and Applications*; Wiley: New York, 2005.

(45) Boukamp, B. A. *Solid State Ionics* **1986**, *20*, 31.

(46) Engelkes, V. B.; Beebe, J. M.; Frisbie, C. D. *J. Am. Chem. Soc.* **2004**, *126*, 14287.

Table 2. Water Contact Angle of the Four Studied SAMs: C10, C16, 11-MUA, and 16-MHDA

monolayers	C10	C16	11-MUA	16-MHDA	16-MHDA (acid + KOH)
contact angle (deg)	109 ± 2	111 ± 2	<10	<12	<12

Such behavior is in agreement with strongly hydrophilic surfaces and suggests that both 11-MUA and 16-MHDA self-assemble on the substrate with their acid groups oriented toward the air side.[8] The water contact angle of the 16-MHDA SAMs prepared with acetic acid and KOH is also very low, consistent with the ionic nature of the surface. Contact angle measurements of 16-MHDA prepared only with ethanol or with ethanol + acetic acid and rinsed with KOH do not manifest any difference in terms of wettability.

The results of Table 2 are in good agreement with previously reported values,[8] but they differ from the results of other authors,[24,47] who found the contact angles of carboxylic-terminated SAMs prepared only with ethanol to be higher. We observed that contact angles of carboxylic-terminated SAMs can be a few degrees higher than those presented in Table 2 if freshly prepared samples are measured too soon, i.e., before they are completely dry. Additionally, we noticed that the roughness of the gold substrate influences the quality of the monolayer. Thus, solvent contamination or differences in substrate roughness can explain discrepancies in contact angle data reported in other publications.

Conclusions

We have investigated acid- and methyl-terminated self-assembled monolayers of alkanethiols with different alkyl chain length. C10, C16, 11-MUA, and 16-MHDA on Au(111) were characterized by STM, XPS, and contact angle measurements. Molecular resolution STM images of C16 were achieved for the first time, and both C10 and C16 show ordered domains with $(\sqrt{3} \times \sqrt{3})R30°$ lattice and a $c(4 \times 2)$ superstructure. In contrast, 11-MUA monolayers form smaller ordered domains than *n*-alkanethiols, and regions with a simple $(\sqrt{3} \times \sqrt{3})R30°$ lattice, a $c(4 \times 2)$ superlattice, and nonordered arrangements coexist on the surface. Finally, 16-MHDA presents the morphology of a uniform alkanethiol monolayer with the characteristic single-atom-deep etch pits. In this case, both the thickness of the monolayer and the hydrophilic properties of the surface make it impossible to reach molecular resolution in air. XPS spectra showed peak positions and line shapes in agreement with the chemical structure of the molecules. The film thicknesses, estimated by both XPS and electrochemistry, are in good agreement with the values expected taking into account the C−C distance in the alkyl chain and fully extended alkanethiols tilted by 30° with respect to the substrate normal. Furthermore, despite the presence of a small fraction of pinholes (surface coverage ≤0.2%), the films proved to act as an effective barrier to both ion penetration and electron transfer to/from solution redox probes. The water contact angles of methyl-terminated monolayers were very high (∼110°) because methyl groups create extremely hydrophobic surfaces. In contrast, acid-terminated monolayers presented very low water contact angles (<12°) as expected for highly hydrophilic surfaces formed when most of the acid groups of 11-MUA and 16-MHDA point upright. 16-MHDA monolayers prepared only with ethanolic solution are as good and uniform as the ones prepared with acetic acid/ethanol and additionally rinsed in KOH. Furthermore, the acetic acid was difficult to remove and appears as contamination on the surface. Hence, we have demonstrated that ordered acid-terminated alkanethiol self-assembled monolayer can be obtained with the same preparation conditions used for methyl-terminated ones, without any other particular treatment.

Acknowledgment. This work was performed within the EU RT network EMMMA Contract No. HPRN-CT-2002-00168 and the EU Contracts MECHMOL No. IST-2001-35504 and Hy3M No. NMP4-CT-2004-013525. This project received additional support from the Dutch Foundation for Fundamental Research on Matter (FOM), from the Breedtestrategie program of the University of Groningen, and from the Italian MIUR and the University of Bologna.

LA0605539

(47) Michael, K.; Vernekar, V.; Keselowsky, B.; Meredith, J. Latour, R.; Garcia, A. *Langmuir* **2003**, *19*, 8033.